

Zn(II), Ni(II), Cu(II), and Fe(III) Complexes of Potentially Bimetalating Tris(pyridine- and imidazole-appended) Picket-Fence Naphthylporphyrins with Benzyl Ether Spacers: Implications for Cytochrome *c* Oxidase Active-Site Modeling

Thomas P. Thrash and Lon J. Wilson*

Department of Chemistry and the Center for Nanoscale Science and Technology, M.S. 60, Rice University, P.O. Box 1892, Houston, Texas 77251-1892

Received September 28, 2000

Two new unsymmetrical picket-fence naphthylporphyrin ligands, **1** and **2**, and several of their metalated porphyrinato complexes have been synthesized as precursor model compounds for the binuclear (Fe/Cu) cytochrome *c* oxidase (CcO) active site. **1** and **2** have a naphthylporphyrin superstructure that has been specifically incorporated to confer long-term configurational stability to the atropisomeric products. The two picket-fence porphyrin ligands also bear covalently linked, axially offset tris(heterocycle) coordination sites for a copper ion, much like that found in the native enzyme. Monometallic porphyrin complexes [M = Zn(II), Ni(II), Cu(II), and Fe(III)] of the pyridine-appended ligand **1** have been prepared and spectroscopically and magnetically characterized. An unusual monomeric iron(III) hydroxo porphyrin complex was isolated upon workup of the compound formed under ferrous sulfate/acetic acid reflux conditions. There is general difficulty in forming binuclear complexes of **1**, which is attributed to the conformational flexibility of the benzyl ether type picket spacers. The potential of ligands such as **1** and **2** for future CcO active-site modeling studies is considered.

Introduction

Cytochrome *c* oxidase (CcO) is the terminal enzyme in the biological electron-transport cycle, catalyzing the four-electron reduction of dioxygen into two molecules of water.^{1–3} The energy liberated by this exergonic reaction is utilized by ATP synthase to drive the conversion of ADP and inorganic phosphate into ATP. Efforts toward understanding the enzymatic mechanism have recently advanced significantly with reports of the whole enzyme X-ray structures from mammalian^{4–6} and bacterial^{7–9} sources. These 2.8 Å or better resolution X-ray structures confirmed several structural features that had long been proposed on the basis of spectroscopic evidence, particularly EXAFS^{10–15} and EPR/ENDOR.^{16,17}

The CcO X-ray structures revealed at least seven metal atoms in the resting (oxidized) enzyme: a binuclear, mixed-valence copper(I/II) site [Cu_A], an isolated low-spin iron(III) porphyrin [heme a], a high-spin iron(III) porphyrin [heme a₃] with a closely positioned, monomeric copper(II) center [Cu_B], and, finally, redox-inactive magnesium(II) and zinc(II) sites.^{4,5,7,8} The structures of the fully reduced and azide- and CO-bound enzyme have also recently been reported.^{6,9} The likely electron-transfer route is cytochrome *c* → Cu_A → heme a → heme a₃/Cu_B → H₂O. The oxidized active-site structure (Figure 1) consists of an Fe(III) heme having an axially bound histidine imidazole ligand. The nearby Cu_B is a Cu(II) center coordinated by three histidine imidazole nitrogens. The Cu_B atom is located ~4.5 Å from the heme a₃ iron and is displaced ~1 Å from the heme perpendicular microsymmetry axis toward the histidines. None of the X-ray structural studies definitively located a bridging ligand between the active-site metal centers. This finding is surprising, since strong antiferromagnetic coupling exists in the native enzyme to form an overall *S* = 2, EPR-silent state.^{1–3,18,19} EXAFS studies have suggested bridging atoms such as S or Cl,^{10–15} and other ligands have been postulated as well (oxo, hydroxo, histidyl).²⁰

* To whom correspondence should be addressed.

- (1) Chan, S. I.; Li, P. M. *Biochemistry* **1990**, *29*, 1.
- (2) Malmström, B. G. *Chem. Rev.* **1990**, *90*, 1247.
- (3) Babcock, G. T.; Wikström, M. *Nature* **1992**, *356*, 301.
- (4) Tsukihara, T.; Aoyama, H.; Yamashita, E.; Tomizaki, T.; Yamaguchi, H.; Shinzawa-Itoh, K.; Nakashima, R.; Yaono, R.; Yoshikawa, S. *Science* **1995**, *269*, 1069.
- (5) Tsukihara, T.; Aoyama, H.; Yamashita, E.; Tomizaki, T.; Yamaguchi, H.; Shinzawa-Itoh, K.; Nakashima, R.; Yaono, R.; Yoshikawa, S. *Science* **1996**, *272*, 1136.
- (6) Yoshikawa, S.; Shinzawa-Itoh, K.; Nakashima, R.; Yaono, R.; Yamashita, E.; Inoue, N.; Yao, M.; Fei, M. J.; Libeu, C. P.; Mizushima, T.; Yamaguchi, H.; Tomizaki, T.; Tsukihara, T. *Science* **1998**, *280*, 1723.
- (7) Iwata, S.; Ostermeier, C.; Ludwig, B.; Michel, H. *Nature* **1995**, *376*, 660.
- (8) Ostermeier, C.; Harrenga, A.; Ermler, U.; Michel, H. *Proc. Natl. Acad. Sci. U.S.A.* **1997**, *94*, 10547.
- (9) Harrenga, A.; Michel, H. *J. Biol. Chem.* **1999**, *274*, 33296.
- (10) Powers, L.; Chance, B.; Ching, Y.; Angiolillo, P. *Biophys. J.* **1981**, *34*, 465.
- (11) Scott, R. A.; Schwartz, J. R.; Cramer, S. P. *Biochemistry* **1986**, *25*, 5546.
- (12) Li, P. M.; Gelles, J.; Chan, S. I.; Sullivan, R. J.; Scott, R. A. *Biochemistry* **1987**, *26*, 2091.
- (13) Scott, R. A. *Annu. Rev. Biophys. Biophys. Chem.* **1989**, *18*, 137.

- (14) Laureau, M.; Powers, L.; Chance, B.; Wikström, M. *J. Inorg. Biochem.* **1993**, *51*, 274.
- (15) George, G. N.; Cramer, S. P.; Frey, T. G.; Prince, R. C. *Biochim. Biophys. Acta* **1993**, *1142*, 240.
- (16) Stevens, T. H.; Chan, S. I. *J. Biol. Chem.* **1983**, *256*, 1069.
- (17) Cline, J.; Reinhammar, B.; Jensen, P.; Venters, R.; Hoffman, B. M. *J. Biol. Chem.* **1983**, *258*, 5124.
- (18) Tweedle, M. F.; Wilson, L. J.; Garcia-Iñiguez, L.; Babcock, G. T.; Palmer, G. J. *J. Biol. Chem.* **1978**, *253*, 8065.
- (19) Day, E. P.; Peterson, J.; Sendova, M. S.; Schoonover, J.; Palmer, G. *Biochemistry* **1993**, *32*, 7855.
- (20) Karlin, K. D.; Nanthakumar, A.; Fox, S.; Murthy, N. N.; Ravi, N.; Huynh, B. H.; Orosz, R. D.; Day, E. P. *J. Am. Chem. Soc.* **1994**, *116*, 4753.

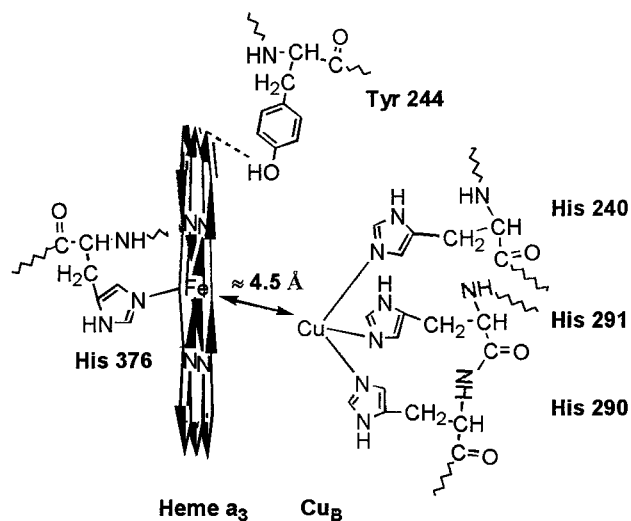


Figure 1. Schematic representation of the resting CcO active-site structure as viewed parallel to the heme a_3 plane. Peripheral side chains of the protoporphyrin IX ligand have been omitted for clarity. The dashed line from Tyr 244 represents a hydrogen bond to a heme a_3 hydroxyfarnesylethyl group (not shown).

The present state of studying metalloenzyme systems with model compounds has been the subject of a recent review.²¹ The CcO active site, in particular, has been the focus of numerous small molecule modeling efforts,^{20,22–45} most of which have utilized picket-fence porphyrin methodology.⁴⁶ Some

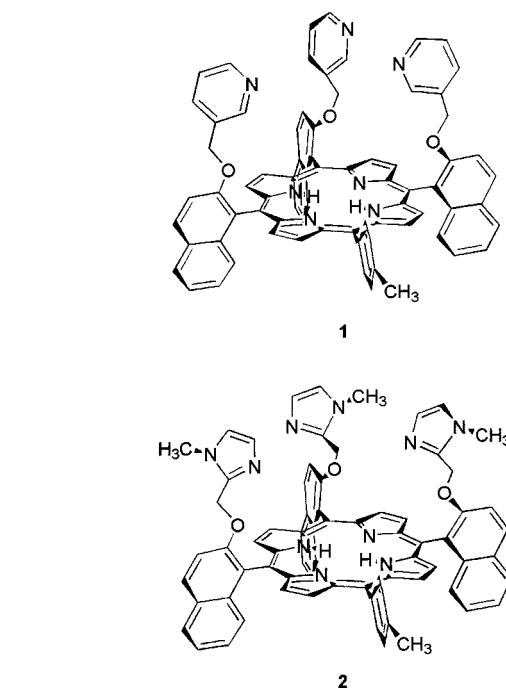


Figure 2. The new tris(picket-fence) porphyrin CcO model compound ligands: $H_2T(NAPOPY)_3P$ (1) and $H_2T(NAPOIM)_3P$ (2).

especially successful approaches toward modeling the CcO active site have recently been disclosed. Collman has reported several CcO model compounds bearing axial imidazole ligands that efficiently perform four-electron dioxygen reduction.^{38,39,41,44} Karlin and Holm have prepared CcO model compounds in which the Cu-binding site is linked to the porphyrin through an unsupported μ -oxo bridge, producing antiferromagnetic coupling between the Fe(III) and Cu(II) centers.^{20,45} A covalently supported version of one of these compounds has also been synthesized.⁴⁷ Finally, it is only recently that the first CcO model compounds bearing imidazoles at the Cu_B -binding site have been reported.^{42–44}

The present work takes a somewhat different approach to CcO active-site modeling with the synthesis of a new class of picket-fence porphyrin compounds. The new ligands **1** and **2** (Figure 2) incorporate several structural features that were predicted to give improved ease of handling, provide for structural flexibility, and accurately reproduce the CcO active-site architecture. First, naphthyl groups have replaced the more typically used phenyl groups in the tetraarylporphyrin superstructure. These sterically encumbered naphthyl moieties block atropisomer interconversion, allowing the desired porphyrin stereoisomer to be isolated and indefinitely retained. Second, an unsymmetrical α,α,α -tris(2-hydroxy-1-naphthyl)porphyrin precursor has been employed to prepare ligands with only three heterocyclic groups above one porphyrin face.^{34–39,41–44} This arrangement also forces the “upstairs” binding site to be located off-axis as in the enzyme. Finally, a benzyl ether type OCH_2 spacer has been utilized for the first time to promote a conformationally flexible upstairs metal site with a probable short metal (porphyrin)–metal (heterocycle) distance ($<5 \text{ \AA}$), in contrast to the rigidity introduced by the more typically used amide spacers which may promote longer $M-M'$ distances. Preparation and characterization of picket-fence porphyrins **1** and **2** and several monometallic [Zn(II), Ni(II), Cu(II), and Fe-

- (21) Collman, J. P. *Inorg. Chem.* **1997**, *36*, 5145.
 (22) Elliott, C. M. *J. Chem. Soc., Chem. Commun.* **1978**, 399.
 (23) Buckingham, D. A.; Gunter, M. J.; Mander, L. N. *J. Am. Chem. Soc.* **1978**, *100*, 2899.
 (24) Gunter, M. J.; Mander, L. N.; McLaughlin, G. M.; Murray, K. S.; Berry, K. J.; Clark, P. E.; Buckingham, D. A. *J. Am. Chem. Soc.* **1980**, *102*, 1470.
 (25) Berry, K. J.; Clark, P. E.; Gunter, M. J.; Murray, K. S. *Nouv. J. Chim.* **1980**, *4*, 581.
 (26) Gunter, M. J.; Mander, L. N.; Murray, K. S. *J. Chem. Soc., Chem. Commun.* **1981**, 799.
 (27) Gunter, M. J.; Berry, K. J.; Murray, K. S. *J. Am. Chem. Soc.* **1984**, *106*, 4227.
 (28) Gunter, M. J.; Mander, L. N.; Murray, K. S.; Clark, P. E. *J. Am. Chem. Soc.* **1981**, *103*, 6784.
 (29) Larsen, N. G.; Boyd, P. D. W.; Rodgers, S. J.; Wuenschell, G. E.; Koch, C. A.; Rasmussen, S.; Tate, J. R.; Erler, B. S.; Reed, C. A. *J. Am. Chem. Soc.* **1986**, *108*, 6950.
 (30) Rodgers, S. J.; Koch, C. A.; Tate, J. R.; Reed, C. A.; Eigenbrot, C. W.; Scheidt, W. R. *Inorg. Chem.* **1987**, *26*, 3647.
 (31) Chang, C. K.; Koo, M. S.; Ward, B. J. *J. Chem. Soc., Chem. Commun.* **1982**, 716.
 (32) Okamoto, M.; Nishida, Y.; Kida, S. *Chem. Lett.* **1982**, 1773.
 (33) Bulach, V.; Mandon, D.; Weiss, R. *Angew. Chem., Int. Ed. Engl.* **1991**, *30*, 572.
 (34) Sasaki, T.; Naruta, Y. *Chem. Lett.* **1995**, 663.
 (35) Casella, L.; Monzani, E.; Gullotti, M.; Gliubich, F.; De Gioia, L. *J. Chem. Soc., Dalton Trans.* **1994**, 3203.
 (36) Fujii, H.; Yoshimura, T.; Kamada, H. *Chem. Lett.* **1996**, 581.
 (37) Bag, N.; Chern, S.-S.; Peng, S.-M.; Chang, C. K. *Inorg. Chem.* **1995**, *34*, 753.
 (38) Collman, J. P.; Herrmann, P. C.; Boitrel, B.; Zhang, X.; Eberspacher, T. A.; Fu, L. *J. Am. Chem. Soc.* **1994**, *116*, 9783.
 (39) Collman, J. P.; Fu, L.; Herrmann, P. C.; Zhang, X. *Science* **1997**, *275*, 949.
 (40) Andrioletti, B.; Ricard, D.; Boitrel, B. *New J. Chem.* **1999**, *23*, 1143.
 (41) Collman, J. P.; Schwenninger, R.; Rapta, M.; Bröring, M.; Fu, L. *J. Chem. Soc., Chem. Commun.* **1999**, 137.
 (42) Baeg, J.-O.; Holm, R. H. *J. Chem. Soc., Chem. Commun.* **1998**, 571.
 (43) Tani, F.; Matsumoto, Y.; Tachi, Y.; Sasaki, T.; Naruta, Y. *J. Chem. Soc., Chem. Commun.* **1998**, 1731.
 (44) Collman, J. P.; Rapta, M.; Bröring, M.; Raptova, L.; Schwenninger, R.; Boitrel, B.; Fu, L.; L'Her, M. *J. Am. Chem. Soc.* **1999**, *121*, 1387.
 (45) Lee, S. C.; Holm, R. H. *J. Am. Chem. Soc.* **1993**, *115*, 11789.
 (46) Collman, J. P.; Gagne, R. R.; Reed, C. A.; Halbert, T. R.; Lang, G.; Robinson, W. T. *J. Am. Chem. Soc.* **1975**, *97*, 1427.

- (47) Obias, H. V.; van Strijdouck, G. P. F.; Lee, D.-H.; Ralle, M.; Blackburn, N. J.; Karlin, K. D. *J. Am. Chem. Soc.* **1998**, *120*, 9696.

(III)] porphyrin complexes of **1** are described in this work as an initial investigation toward the development of picket-fence naphthylporphyrins as CcO active-site model compounds.⁴⁸

Experimental Section

All compounds were reagent grade or better. Pyrrole (Acros) was distilled from CaH₂ under vacuum and stored over 4 Å molecular sieves at -30 °C. The following reagents were used as received: 2-methoxy-1-naphthaldehyde (Aldrich), *p*-tolualdehyde (Aldrich), neat BBr₃ (Aldrich), 3-picoyl chloride hydrochloride (Aldrich), Zn(CF₃SO₃)₂·H₂O (Alfa), Cu(CF₃SO₃)₂ (Aldrich), Ni(CH₃CO₂)₂·4H₂O (Fisher), and FeSO₄·7H₂O (Mallinckrodt). Solvents were used as received, with one exception; for procedures requiring dry CH₂Cl₂, the solvent was refluxed with CaH₂ and then distilled under Ar. Chromatographic separations were accomplished as appropriate on either neutral alumina (Aldrich, Brockmann I, 150 mesh, 58 Å, surface area 155 m² g⁻¹) or silica gel (Aldrich, grade 62, 60–200 mesh, 150 Å). NMR solvents CDCl₃ (Cambridge Isotope Laboratories, 99.8% atom D) and pyridine-*d*₅ (Aldrich, 99% atom D) were used as received.

NMR spectra were obtained on a Bruker Avance 400 MHz or Bruker AF-250 MHz spectrometer. UV-vis characterization was accomplished with a GBC model 918 UV-vis spectrophotometer. Mass spectral analyses were performed on a Finnigan Mat 95 mass spectrometer. Infrared spectra were obtained as KBr disks using a Nicolet Magna-IR 760 spectrometer. Paramagnetic compounds were characterized with a Varian E-Line EPR spectrometer (X-band) and by SQUID magnetometry (Quantum Design, MPMS-5S). Bulk magnetic measurements were corrected by subtracting the experimentally measured diamagnetic contributions from the quartz sample cell and the free ligand. Elemental analyses were obtained commercially from Galbraith Laboratories (Knoxville, TN). Metal analyses were performed either in-house by flame atomic absorption spectroscopy (GBC model 908) or commercially by Galbraith Laboratories. Qualitative elemental composition studies were accomplished by EDS electron microprobe analysis (Cameca SX-50).

α,α,α-5,10,15-Tris(2-hydroxy-1-naphthyl)-20-p-tolylporphyrin, H₂T(NAPOH)₃P. The desired unsymmetrical porphyrin atropisomer was synthesized as a mixture of porphyrin products from a mixed-aldehyde condensation with pyrrole.⁴⁹ In a typical reaction, 14.01 g of 2-methoxy-1-naphthaldehyde (75 mmol), 2.9 mL of *p*-tolualdehyde (25 mmol), and 6.9 mL of pyrrole (100 mmol) were combined in 250 mL of propionic acid and refluxed for 1 h. The propionic acid solvent was then removed under reduced pressure, and the product was chromatographed twice on alumina with CH₂Cl₂ eluent. Separation of the desired atropisomeric product was not possible at this point due to similar polarities of the compounds, and the product mixture (13 porphyrin atropisomers) was used without further purification for the step immediately below. Yield (of mixture): 2.46 g (~10% porphyrins).

The methoxy groups of the product mixture were removed under mild conditions using BBr₃.⁵⁰ In a typical reaction, 6.20 g of the porphyrin mixture was dissolved in 140 mL of dry CH₂Cl₂, and the solution was chilled to -60 °C. A 4.4 mL sample of neat BBr₃ (46.5 mmol, excess) was added dropwise to the cold solution via syringe, during which time the reaction mixture turned green. The solution was maintained at -60 °C for 1 h and then gradually warmed to room temperature overnight. Excess BBr₃ was quenched at that time by slowly adding 50 mL of deionized water to the reaction mixture and vigorously stirring for 15 min. The CH₂Cl₂ solution was diluted with 500 mL of EtOAc and neutralized with three 10% NaHCO₃ washes. The EtOAc extract was then washed twice with deionized water, dried over anhydrous Na₂SO₄, and gravity filtered. The solution was taken to dryness under reduced pressure, and α,α,α-H₂T(NAPOH)₃P was isolated chromatographically as follows. The crude reaction product was dissolved in a minimum amount of CHCl₃ and loaded onto a CHCl₃

slurry-packed silica gel column. As soon as the product was thoroughly adsorbed, the eluent was changed to acetone/hexanes (3:7), and the adsorbed material eluted as a very broad, apparently unresolved, dark red-purple band. Fractions were collected periodically and analyzed by TLC [acetone/hexanes (3:7)] and NMR for product content. Pure α,α,α-H₂T(NAPOH)₃P was obtained as the next-to-last eluted compound (see the Results and Discussion). The desired product eluted between α,α,α,β- and α,α,α,α-5,10,15,20-tetrakis(2-hydroxy-1-naphthyl)porphyrin, H₂THNP. Final purification was achieved by recrystallization from CHCl₃/hexanes. Yield: 0.48 g (0.23% from pyrrole, two steps). ¹H NMR (CDCl₃): δ = 8.88 (d, 2H), 8.69 (d, 2H), 8.60 (m, 4H), 8.24 (t, 3H), 8.05 (m, 5H), 7.60 (m, 5H), 7.37 (m, 3H), 7.05 (t, 3H), 6.90 (t, 3H), 5.10 (br s, 3H), 2.69 (s, 3H), -2.40 (br s, 2H). UV-vis (CH₂Cl₂): 424 (Soret), 516, 548, 589, 644 nm. MS (CI⁺): M + 1 = 827, C₅₇H₃₈N₄O₃ + H.

α,α,α-5,10,15-Tris(2-(3-pyridyl)methyleneoxy-1-naphthyl)-20-p-tolylporphyrin, H₂T(NAPOPY)₃P (1). In a typical reaction, 250 mg of H₂T(NAPOH)₃P (0.3 mmol) and 250 mg of powdered KOH (4.5 mmol, excess) were dissolved in 16 mL of DMSO, and the solution was stirred under Ar for 30 min. A 300 mg sample of 3-picoyl chloride hydrochloride (1.8 mmol) was dissolved in 8 mL of DMSO and added to the reaction mixture. The reaction was stirred at room temperature for 8 h and then poured into 75 mL of deionized water. The porphyrin was extracted into EtOAc, and the extract was then sequentially washed with 1 M NaOH, deionized water, 1 M NaOH, deionized water, and finally saturated aqueous NaCl twice. The solution was dried over anhydrous MgSO₄, gravity filtered, and reduced to dryness. The crude reaction product was dissolved in CHCl₃ and chromatographed on a slurry-packed silica gel column with MeOH/CHCl₃ (1:19). Two narrow red bands moved just behind the solvent front and were followed by a much broader, slower-moving, dark red-purple product band. The product eluent was purified further by recrystallization from CHCl₃/hexanes. Yield: 160 mg (48%). ¹H NMR (CDCl₃): δ = 8.78 (d, 2H), 8.54 (d, 2H), 8.44 (m, 4H), 8.24 (t, 3H), 8.07 (m, 10H), 7.89 (d, 1H), 7.66 (t, 3H), 7.51 (t, 2H), 7.33 (t, 3H), 7.00 (m, 4H), 6.91 (d, 2H), 6.54 (ddt, 2H), 6.38 (m, 3H), 6.18 (dd, 1H), 5.03 (s, 4H), 4.99 (s, 2H), 2.67 (s, 3H), -2.24 (br s, 2H). ¹³C NMR (CDCl₃, selected peaks): δ = 156.13/156.08 (naphthyl, C-2), 148.63/148.55 and 147.91/147.79 (pyridyl, C-2 and C-6), 68.93/68.89 (OCH₂), 21.50 (Ar-CH₃). UV-vis (CH₂Cl₂): 425 (Soret), 516, 550, 591, 646 nm. MS (CI⁺): M + 1 = 1100, C₇₅H₅₃N₇O₃ + H. Anal. Calcd for C₇₅H₅₃N₇O₃·H₂O: C, 80.55; H, 4.96; N, 8.77. Found: C, 80.44; H, 4.97; N, 8.65.

General Procedure for Metalation with Zn(II), Cu(II), and Ni(II): [M^{II}T(NAPOPY)₃P]. Metalation with Zn(II), Cu(II), and Ni(II) was accomplished by refluxing 5–10 equiv of the metal salt (either the triflate or acetate) in an appropriate solvent (either CHCl₃/MeOH or DMF) until UV-vis spectroscopy indicated completion of the reaction. At this point, the solvent was removed under reduced pressure, and the residue was redissolved in CHCl₃ and washed with deionized water several times to remove excess metal salt. The CHCl₃ solution was reduced to dryness, and the metalated porphyrin product was recrystallized from CHCl₃/hexanes. Full experimental details and data can be found in the Supporting Information.

α,α,α-5,10,15-Tris(2-(3-pyridyl)methyleneoxy-1-naphthyl)-20-p-tolylporphyrinatoiron(III) Hydroxide, [Fe^{III}T(NAPOPY)₃P(OH)]. Metalation with iron was accomplished by a modification of the ferrous sulfate/acetic acid method.⁵¹ A 110 mg sample of **1** (0.10 mmol) was dissolved in 55 mL of glacial acetic acid, and 280 mg of FeSO₄·7H₂O (1.0 mmol) was added. The solution was refluxed in air for 1 h, cooled, and then reduced to dryness under vacuum. The green-brown residue was partitioned between CHCl₃ and deionized water with the aid of brief sonication, and the organic phase was then washed five times with deionized water. The CHCl₃ solution was gravity filtered after extraction, and some residual brown-black particulates were discarded. The filtered solution was reduced to dryness, dried further under vacuum, and recrystallized from CHCl₃/hexanes. The product was homogeneous by TLC [MeOH/CHCl₃ (1:19)]. Yield: 95 mg (78%).

(48) Harmjanz, M.; Scott, M. J. *J. Chem. Soc., Chem. Commun.* **2000**, 397.

(49) Adler, A. D.; Longo, F. R.; Finarelli, J. D.; Goldmacher, J.; Assour, J.; Korsakoff, L. *J. Org. Chem.* **1967**, *32*, 476.

(50) Stäubli, B.; Fretz, H.; Piantini, U.; Woggon, W.-D. *Helv. Chim. Acta* **1987**, *70*, 1173.

(51) Fuhrhop, J.-H.; Smith, K. H. In *Porphyrins and Metalloporphyrins*; Smith, K. M., Ed.; Elsevier: Amsterdam, 1975; p 803.

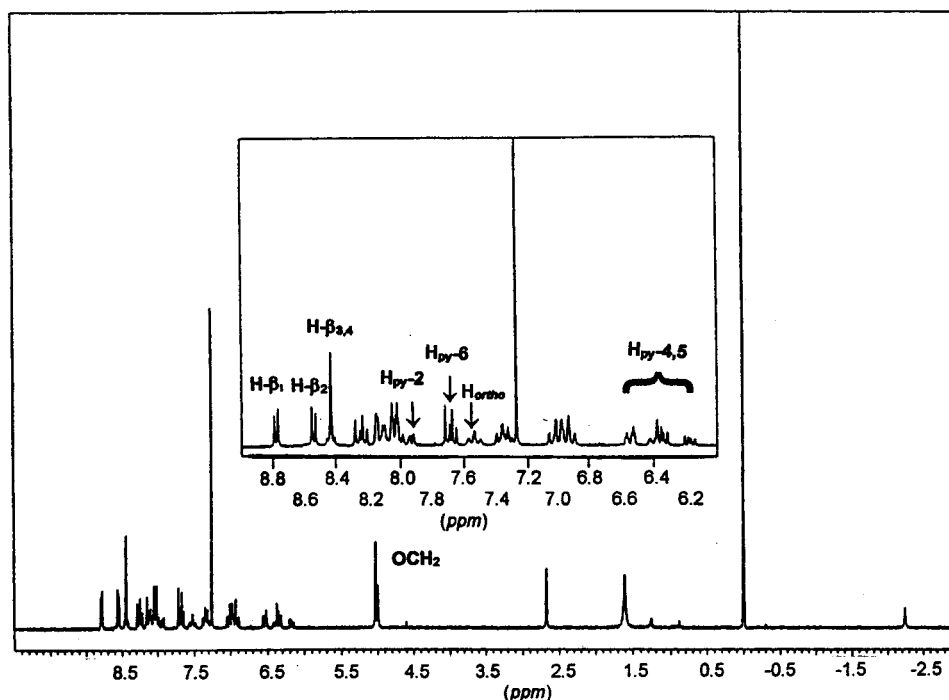


Figure 3. ^1H NMR spectrum of $\text{H}_2\text{T}(\text{NAPOPY})_3\text{P}$ at 400 MHz. The inset is an expansion of the 9.0–6.0 ppm region.

UV-vis (CH_2Cl_2): 334, 421 (Soret), 507 (sh), 576, 630 (sh) nm. EPR (CH_2Cl_2 , 11 K): $g_{\perp} = 5.87$, $g_{\parallel} = 2.03$. Magnetism (1.7–300 K, 1 T): $\mu_{\text{eff}}(300 \text{ K}) = 5.11 \mu_{\text{B}}$. Paramagnetic ^1H NMR (CDCl_3): $\delta = 80$ (br, H- β). MS (CI $^+$): $M + 1 = 1153$, $\text{C}_{75}\text{H}_{51}\text{N}_7\text{O}_3\text{Fe} + \text{H}$. MS (FAB $^+$, 3-nitrobenzyl alcohol matrix): $M + 1 = 1170$, $\text{C}_{75}\text{H}_{52}\text{N}_7\text{O}_4\text{Fe} + \text{H}$. Anal. Calcd for $\text{C}_{75}\text{H}_{52}\text{N}_7\text{O}_4\text{Fe} \cdot 3\text{H}_2\text{O}$: C, 73.53; H, 4.77; N, 8.00; Fe, 4.56. Found: C, 73.02; H, 4.41; N, 7.87; Fe, 4.40. Acetate by ion chromatography: found only 0.21.

Results and Discussion

Ligand Synthesis. Picket-fence naphthylporphyrin ligands **1** and **2** were synthesized in three steps from commercially available starting materials. The desired atropisomeric porphyrin scaffold was obtained as an inseparable mixture of porphyrin products and atropisomers from a mixed-aldehyde condensation with pyrrole. However, the α,α,α -configuration triphenolic porphyrin $\text{H}_2\text{T}(\text{NAPOH})_3\text{P}$ was easily isolated after demethylation. The product configuration was established on the basis of the compound's polarity and relative elution position between two highly polar $\text{H}_2\text{T}(\text{NHP})$ atropisomers whose configurations are readily established by ^1H NMR spectroscopy.⁵² Further evidence of the product configuration was provided by the peak symmetry pattern in the ^1H and ^{13}C NMR spectra of **1** as discussed in more detail below.

No evidence of atropisomer interconversion was observed for the solid α,α,α - $\text{H}_2\text{T}(\text{NAPOH})_3\text{P}$ intermediate over one year of storage at room temperature or for any derived reaction product. The absence of atropisomer interconversion attests to the usefulness of naphthyl picket-fence porphyrins for preparing CcO model compound ligands. Both **1** and **2** were prepared in good yields via nucleophilic displacement at a benzylic center. Difficulty in handling the light-sensitive, imidazole-appended porphyrin^{53,54} **2**, however, led to most studies being performed

on **1** for this initial investigation. The synthesis and characterization of **2** can be found in the Supporting Information.

The unsymmetrical *meso* substitution pattern of **1** is displayed by its ^1H NMR H- β splitting pattern (Figure 3). The β protons adjacent to the tolyl group appear as a resolved downfield doublet at 8.78 ppm (H- β_1), whereas those whose nearest neighbor is a naphthyl group and second-nearest neighbor is the tolyl group occur as a doublet at 8.54 ppm (H- β_2). The β protons whose both nearest and second-nearest neighbors are naphthyl groups occur as overlapping doublets at 8.44 ppm (H- $\beta_{3,4}$). Thus, H- β_1 most resembles the β protons in 5,10,15,20-tetrakis(*p*-tolyl)porphyrin (8.85 ppm, singlet), and H- $\beta_{3,4}$ are similar in H- β resonance position to a H_2TMNP atropisomeric mixture (8.42 ppm, multiplet).⁵² The upfield shifts of the β protons near the naphthyl groups are consistent with increased disruption of the porphyrin ring current by the bulky naphthyl rings, compared to that produced by the relatively unencumbered phenyl substituent.⁵⁵

The α,α,α -configuration of **1** is fully consistent with the ^1H and selected ^{13}C NMR data. Neither ^1H nor ^{13}C NMR spectroscopy can conclusively distinguish between the α,α,α - and α,β,α -configurations, regardless of the field strength, since these two atropisomers are differentiated only by the configuration of the unique naphthyl picket on the symmetry plane. Furthermore, no NOE experiment can distinguish between the two configurations either. However, the high polarity of the $\text{H}_2\text{T}(\text{NAPOH})_3\text{P}$ precursor and its observed elution position in the *predicted* location between α,α,α - and $\alpha,\alpha,\alpha,\beta$ - H_2THNP offer convincing evidence of the proposed configuration assignment (polarity order: $\alpha,\alpha,\alpha,\alpha > \alpha,\alpha,\alpha > \alpha,\alpha,\alpha,\beta > \alpha,\beta,\alpha$). Repeated attempts for more than one year to crystallize **1** and its metalated products for single-crystal X-ray structural analysis have been unsuccessful to date.

The inequivalence of one picket arm is manifested in the narrowly separated ^1H NMR resonances of the benzylic and

(52) Abraham, R. J.; Plant, J.; Bedford, G. R. *Org. Magn. Reson.* **1982**, *19*, 204.

(53) Tsuchida, E.; Komatsu, T.; Arai, K.; Nishide, H. *J. Chem. Soc., Dalton Trans.* **1993**, 2465.

(54) Grimmett, M. R. In *Comprehensive Heterocyclic Chemistry*; Katritzky, A. R., Rees, C. W., Eds.; Pergamon: Oxford, 1984; Vol. 5, p 420.

(55) Janson, T. R.; Katz, J. J. In *The Porphyrins*; Dolphin, D., Ed.; Academic: New York, 1979; Vol. IV, p 28.

pyridyl protons, as well as for selected ^{13}C signals (see the Experimental Section). The benzyl methylene protons appear as two resolved singlets (2:1 integral ratio) near 5 ppm, demonstrating this inequivalence. Likewise, the corresponding carbon signals occur as narrowly separated peaks in approximately a 2:1 intensity ratio. Although the benzylic ^1H resonances occur as singlets in **1**, diastereotopic splitting of these protons was seen in the imidazole-appended ligand **2** at room temperature. Similar diastereotopic methylene splitting has been previously observed in a picket-fence porphyrin, but only at reduced temperatures.²⁹

The pyridine ^1H resonances display upfield and downfield shifts relative to the unappended heterocycle, since these protons lie in both the shielding and deshielding regions of the porphyrin ring current. Further, slight chemical shift differences for one set of resonances again indicate the presence of the unique pyridine ring. The pyridine H-2 protons ($\text{H}_{\text{py}-2}$) are manifested as narrowly split doublets at 8.07 and 7.89 ppm. The downfield signal is obscured by the naphthyl H-3/H-5/*m*-tolyl multiplet, but integration places the two additional protons under this peak. The higher field signal integrates to one proton, and the narrow doublet is consistent with long-range coupling to H-4. The overlapping doublets (2:1 integral ratio) at 7.66 ppm may be attributed to the pyridine H-6 resonances ($\text{H}_{\text{py}-6}$), leaving the three far-upfield-shifted signals (6.54, 6.38, and 6.18 ppm) assignable to the inequivalent sets of pyridine ring H-4 and H-5 protons ($\text{H}_{\text{py}-4,5}$). The proton resonances for the pyridine on the symmetry plane all lie slightly farther upfield than do those of the symmetry-related rings. The narrowly separated ^{13}C NMR resonances of the pyridine C-2 and C-6 positions also display peak height intensity ratios of approximately 2:1, again demonstrating the inequivalence of one picket arm.

One interesting NMR spectroscopic feature of **1** that deserves special mention is the splitting pattern of its *o*-tolyl protons. The *m*-tolyl signals are hidden beneath the multiplet at 8.07 ppm, but the *o*-tolyl protons (H_{ortho}) are clearly observed at 7.51 ppm. The *ortho* protons are assigned as the upfield signal, since they are more shielded by the porphyrin ring current. Instead of the expected doublet, however, an apparent triplet is observed. The "triplet" is actually, upon careful observation, a set of overlapping doublets. Slow tolyl group rotation evidently distinguishes the protons above the α and β porphyrin faces, resulting in the overlapping doublets. Very slight peak broadening is also consistent with this assessment. Similar slow rotation of unhindered porphyrin aryl groups (such as *p*-tolyl) has recently been noted.⁵⁶

Monometallic Zn(II), Cu(II), and Ni(II) Complexes. Before preparation of any Fe(III) compound, the homobimetallic Zn(II), Ni(II), and Cu(II) complexes of **1** were initially pursued as simpler reference compounds. In addition, it was hoped that the solution-state Cu(II)–Cu(II) distance could be indirectly determined in the dicopper complex through use of the EPR dipolar coupling constant.^{40,57,58}

Zn(II) metalation of **1** proceeded readily as determined by UV–vis spectroscopy. However, upon workup of the reaction mixture, a very broad ^1H NMR spectrum was obtained in CDCl_3 at room temperature. Metalation under various conditions, including use of counteranions other than triflate (acetate or

chloride), failed to produce any changes in the NMR spectrum. In contrast to the broad ^1H NMR spectrum in CDCl_3 , $[\text{Zn}^{\text{II}}\text{T}(\text{NAPOPY})_3\text{P}]$ gave a spectrum with very sharp signals in pyridine-*d*₅. These results can be rationalized as follows.

Zinc(II) porphyrins are either four- or five-coordinate, with a loosely held, neutral ligand sometimes filling the axial coordination position.^{59,60} In pyridine-*d*₅, the ligating bulk solvent fully occupies the axial coordination site, and the observed spectrum is that of the axial pyridine-*d*₅ complex. In CDCl_3 this site is open, and intermolecular axial coordination of the appended pyridines is apparently more favored than is intramolecular chelation of a second metal at the tris(3-pyridyl) site. Intermolecular ligation results in transient oligomer formation in solution, producing the broad proton resonances. Intramolecular coordination of the appended pyridines is not possible, since the OCH_2 picket spacer is too short to reach the metal site within the same porphyrin. The five-coordinate nature of the Zn(II) complex is supported by its UV–vis spectrum in CH_2Cl_2 ($\alpha:\beta$ intensity ratio 0.37), since ratios greater than 0.25 are typically indicative of axial coordination.⁵⁹ To our knowledge, intermolecular oligomerization has not been previously noted in Zn(II)-metalated picket-fence porphyrin CcO model compounds.

With the realization that bimetallic complex formation was apparently being impeded by competitive oligomerization in the five-coordinate zinc(II) porphyrins, efforts refocused on the Ni(II) and Cu(II) complexes, which are usually only four-coordinate porphyrin species.⁶⁰ It was hoped that, by freeing the heterocyclic pickets from intermolecular coordination, they would readily chelate and form intramolecular bimetallic complexes. As expected, $[\text{Ni}^{\text{II}}\text{T}(\text{NAPOPY})_3\text{P}]$ was easily formed, and its ^1H NMR spectrum in CDCl_3 was sharp and readily assigned to a monomeric metalloporphyrin structure. Interestingly, the *o*-tolyl proton resonance occurs as the expected doublet here, instead of the "triplet" observed for the free ligand, indicating an increased rate of phenyl ring rotation in the metalated compound.

Various mass spectrometry techniques gave parent-ion masses for only the monometallic Zn(II), Ni(II), and Cu(II) complexes of **1** (see the Experimental Section). Bimetallic metalloporphyrin compounds have sometimes failed to display bimetallic parent-ion mass peaks;^{23,28,31,37,61} however, elemental analyses clearly demonstrated that the Ni(II) and Cu(II) compounds were only monometallic. Further treatment of the mononuclear Ni(II) complex with various salts of Ni(II), Cu(II), Zn(II), and Co(II) under mild conditions (stoichiometric to excess metal cation, $\text{CHCl}_3/\text{MeOH}$, room temperature, aqueous workup) failed to produce any changes in the ^1H NMR spectrum, such as paramagnetic broadening or conformationally induced shifts. Also, EDS electron microprobe analysis did not detect even traces of the new metals in the retreated compounds.

All spectral properties of the Cu(II) complex of **1** were also consistent with only a mononuclear formulation. The EPR spectrum of $[\text{Cu}^{\text{II}}\text{T}(\text{NAPOPY})_3\text{P}]$ showed no evidence for a triplet state, which is indicative of a bimetallic Cu(II) compound.^{57,58} The EPR spectrum of $[\text{Cu}^{\text{II}}\text{T}(\text{NAPOPY})_3\text{P}]$ in a frozen CH_2Cl_2 solution at 11 K was characteristic of copper(II) porphyrins and displayed typical anisotropic *g* values ($g_{\parallel} = 2.23$, $g_{\perp} \approx 2.05$).⁶² The bulk magnetic properties of the Cu(II)

(56) Koerner, R.; Wright, J. L.; Ding, X. D.; Nasset, M. J. M.; Aubrecht, K.; Watson, R. A.; Barber, R. A.; Mink, L. M.; Tipton, A. R.; Norvell, C. J.; Skidmore, K.; Simonis, U.; Walker, F. A. *Inorg. Chem.* **1998**, *37*, 733.

(57) Smith, T. D.; Pilbrow, J. R. *Coord. Chem. Rev.* **1974**, *13*, 173.

(58) Eaton, S. S.; More, K. M.; Sawant, B. M.; Eaton, G. R. *J. Am. Chem. Soc.* **1983**, *105*, 6560.

(59) Nappa, M.; Valentine, J. S. *J. Am. Chem. Soc.* **1978**, *100*, 5075.

(60) Buchler, J. W. In *The Porphyrins*; Dolphin, D., Ed.; Academic: New York, 1979; Vol. I, p 425.

(61) Woo, L. K.; Maurya, M. R.; Jacobson, R. A.; Yang, S.; Ringrose, S. L. *Inorg. Chem.* **1992**, *31*, 913.

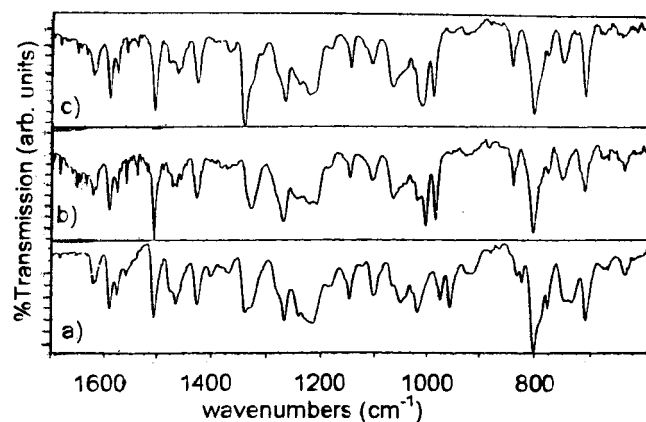


Figure 4. Comparative infrared spectra of $\text{H}_2\text{T}(\text{NAPOPY})_3\text{P}$ (a), $[\text{Ni}^{\text{II}}\text{T}(\text{NAPOPY})_3\text{P}]$ (b), and $[\text{Fe}^{\text{III}}\text{T}(\text{NAPOPY})_3\text{P}(\text{OH})]$ (c).

complex were also consistent with only a mononuclear compound having simple Curie-like behavior from 1.7 to 150 K ($\mu_{\text{eff}} = 1.69 \mu_{\text{B}}$ at 150 K; see Table S-1 in the Supporting Information).

The lack of binuclear compound formation in the Zn(II), Ni(II), and Cu(II) complexes of **1** can likely be attributed to conformational flexibility of the benzyl ether picket spacers. Previous CcO model picket-fence porphyrin ligands have utilized more rigid amide spacers or preformed cyclic chelating sites to encourage a favorable ligand configuration for binding of a second metal. The present model compounds are the first to lack both of these features. Originally, it was hoped that the OCH_2 spacer flexibility would lead to a “conformationally relaxed” heterocyclic binding site (with an especially short metal–metal distance) without having detrimental effects on its chelating ability. Instead, the entropy of these spacer groups is apparently so great that a configuration favorable for chelation is never attained. The absence of binuclear compounds is *not* likely explained by an incorrect atropisomer assignment. As discussed above, the α,α,α -configuration is strongly implicated by elution characteristics, although the α,β,α -configuration cannot be conclusively disproven by NMR spectroscopy. Even in the event of an incorrect configuration assignment, the *trans*-5,15-(3-pyridyl) pickets of the α,β,α -isomer could still coordinate to a second metal atom if binuclear compound formation were at all feasible. Similar *trans*-5,15-binding of Cu(I) has been reported for an amide-linked picket-fence porphyrin model compound.²⁹

Fe(III) Complexes. The mononuclear Fe(III) complex of **1** was also readily prepared by the ferrous sulfate/acetic acid method. Unlike the other mononuclear porphyrin compounds, however, the Fe(III) complex displayed several unanticipated characteristics.

The iron(III) porphyrin compound isolated upon workup of the metalation reaction is apparently the axial hydroxide complex instead of the anticipated acetate compound. This assignment was established on the basis of several independent techniques. First, the infrared spectrum of $[\text{Fe}^{\text{III}}\text{T}(\text{NAPOPY})_3\text{P}(\text{OH})]$ was nearly identical to those of ligand **1** and the analogous Ni(II) complex (Figure 4). This fact leads to two important conclusions: (1) The axial ligand cannot be acetate, since a strong carbonyl stretch is not present near 1650 cm^{-1} , as displayed in other iron(III) acetato porphyrins.⁶³ (2) The product is also most likely not a μ -oxo dimer, as evidenced by the

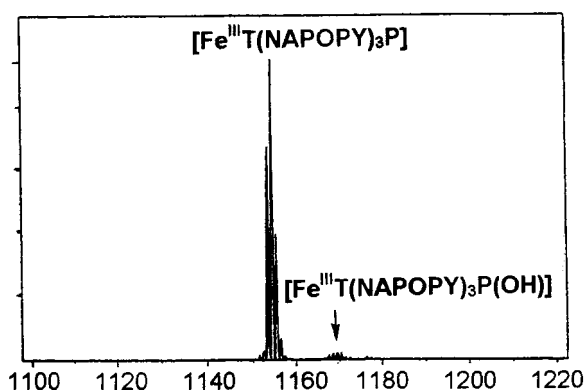


Figure 5. Positive-ion FAB mass spectrum of $[\text{Fe}^{\text{III}}\text{T}(\text{NAPOPY})_3\text{P}(\text{OH})]$.

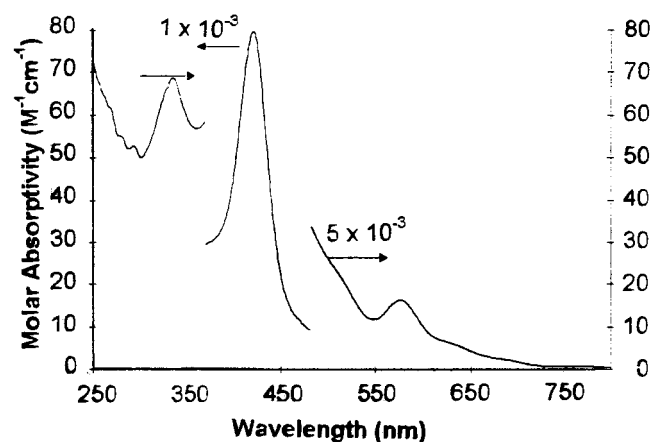


Figure 6. UV-vis spectrum of $[\text{Fe}^{\text{III}}\text{T}(\text{NAPOPY})_3\text{P}(\text{OH})]$ in CH_2Cl_2 .

absence of any new Fe–O–Fe antisymmetric stretching bands in the $850\text{--}900 \text{ cm}^{-1}$ region of the spectrum.⁶⁴ Sulfur-based axial ligands were similarly excluded on the basis of the infrared spectrum, as well as by EDS electron microprobe analysis. This process of elimination leaves hydroxide as the only remaining axial ligand choice, but its existence can be only indirectly inferred from the infrared spectrum, since its OH stretching frequency is coincident with that of bulk water. The absence of an acetate ligand has also been directly established through a negligible ion-chromatography acetate analysis (see the Experimental Section).

Like the other mononuclear porphyrins, $[\text{Fe}^{\text{III}}\text{T}(\text{NAPOPY})_3\text{P}(\text{OH})]$ readily gave a $M + 1 = 1153$ parent ion by positive-ion chemical ionization mass spectrometry, with the axial ligand being lost during the ionization process. However, in contrast to the chemical ionization mass spectrum, the positive-ion FAB mass spectrum showed a weak $M + 1$ parent-ion peak at 1170 mass units for the axial hydroxide complex, as well as a much more intense signal for the ligandless parent ion (Figure 5). Detection of an intact axial hydroxide porphyrin complex by mass spectrometry has not been reported for other known iron(III) hydroxo porphyrin compounds.

The electronic spectrum of $[\text{Fe}^{\text{III}}\text{T}(\text{NAPOPY})_3\text{P}(\text{OH})]$ is also consistent with the axial ligand assignment (Figure 6). The relatively featureless visible region of the spectrum is in good qualitative agreement with those previously reported for iron(III) hydroxo porphyrins.^{26,28,65–73} Typically, the visible region

(62) Assour, J. M. *J. Chem. Phys.* **1965**, *43*, 2477.

(63) Oumous, H.; Lecomte, C.; Protas, J.; Cocolios, P.; Guillard, R. *Polyhedron* **1984**, *3*, 651.

(64) White, W. I. In *The Porphyrins*; Dolphin, D., Ed.; Academic: New York, 1979; Vol. V, p 318.

(65) Amundsen, A. R.; Vaska, L. *Inorg. Chim. Acta* **1975**, *14*, L49.

(66) Cense, J.-M.; Le Quan, R.-M. *Tetrahedron Lett.* **1979**, 3725.

is somewhat better defined for the μ -oxo dimer in those systems which can exist in either the μ -oxo or hydroxo form. The band near 334 nm is also characteristic of only the previously reported iron(III) hydroxo porphyrins.

The CH_2Cl_2 frozen solution EPR spectrum of $[\text{Fe}^{\text{III}}\text{T}(\text{NAPOPY})_3\text{P}(\text{OH})]$ at 11 K showed typical behavior for an axially symmetric, high-spin iron(III) porphyrin compound, with g_{\perp} and g_{\parallel} values of 5.87 and 2.03, respectively. Similarly, the paramagnetic ^1H NMR spectrum of $[\text{Fe}^{\text{III}}\text{T}(\text{NAPOPY})_3\text{P}(\text{OH})]$ in CDCl_3 was also consistent with an $S = 5/2$ high-spin assignment for Fe(III) as evidenced, for example, by its broad H- β resonances centered near 80 ppm (see the Experimental Section). In the solid state, however, the bulk magnetic properties demonstrated considerable deviation from pure $S = 5/2$ high-spin Fe(III) character. At an applied field of 1 T, the room-temperature effective magnetic moment of $[\text{Fe}^{\text{III}}\text{T}(\text{NAPOPY})_3\text{P}(\text{OH})]$ was only $5.11 \mu_{\text{B}}$, compared to typical values of $5.7\text{--}5.9 \mu_{\text{B}}$ for $S = 5/2$ iron(III) porphyrins.⁷⁴ The magnetic moment versus temperature curve reached a maximum near 80 K, before declining slightly to the room-temperature value. Zero-field splitting of the Fe(III) center accounts for a substantial drop in the magnetic moment below 20 K.⁷⁵ The full temperature data (1.7–300 K; see Table S-2 in the Supporting Information) also exclude the possibility that an Fe(III) spin-equilibrium process gives rise to the low observed room-temperature magnetic moment.⁷⁶ Such a spin-equilibrium situation is known to exist in ferric myoglobin hydroxide.^{77,78} Similarly, the proximity of the EPR g_{\perp} value to “6” eliminates the possibility of an $S = 5/2, 3/2$ quantum mechanically admixed state leading to the low magnetic moment.⁷⁹

Magnetic moments below the characteristic values for an $S = 5/2$ spin state have been previously noted in the Fe(III) complexes of a tetrakis(pyridine)-appended picket-fence porphyrin, and the measured moments are extremely sensitive to the identity of the axial ligand and presence of admixed crystallization solvents.⁸⁰ For example, in the stated literature case the room-temperature magnetic moments range from as low as $5.17 \mu_{\text{B}}$ for the axial bromide complex to a near spin-only value of $5.88 \mu_{\text{B}}$ for the axial hydroxide complex. A related dependence on axial ligand identity was apparently seen in the present study. As discussed previously, the axial iron(III) hydroxo complex of **1** demonstrated a substantially depressed magnetic moment. In comparison, when the axial iron(III) chloro complex of **1** was prepared by standard methods,⁸¹ simple spin-

only magnetic properties were seen (i.e., $\mu_{\text{eff}} = 5.9 \mu_{\text{B}}$ at 300 K, data not shown).⁷⁴ The low magnetic moments of the Fe(III) complexes in the literature tetrakis(pyridine) system were attributed to “weakly coupled interactions” in the polymeric solid-state structure.⁸⁰ The magnetic moments of previously reported iron(III) hydroxo porphyrins have typically been in the usual range for high-spin $S = 5/2$ iron(III) porphyrins, except for one compound with a room-temperature magnetic moment of only $5.1 \mu_{\text{B}}$.⁶⁵

Aside from its notable spectroscopic and magnetic properties, $[\text{Fe}^{\text{III}}\text{T}(\text{NAPOPY})_3\text{P}(\text{OH})]$ is also unusual for other reasons. The fact that it exists in the hydroxide-ligated form and shows no tendency to form a μ -oxo dimer is typical of other bifacially encumbered iron(III) porphyrins.^{65–68,70,72,73} **1** has both a proximal face protected by the appended pyridines and a distal face blocked by the naphthyl rings. These two structural features likely explain the easy formation and stability of the iron(III) hydroxo porphyrin, but the fact that the hydroxide form is assumed “spontaneously” upon workup of the metalation reaction is unprecedented. The axial acetate ligand is evidently lost during aqueous workup and replaced by adventitious hydroxide generated in the bulk solvent. Space-filling molecular models indicate that the acetate anion may fit poorly into the binding pocket, potentially explaining its easy loss. Admixed water in the CHCl_3 extraction solvent ($\sim 1\%$ H_2O) and the enhanced basicity of the alkyl-substituted pyridine moieties are evidently sufficient to produce enough hydroxide to effect ligand exchange for the weakly bound acetate. The significantly different physical properties of the chloride and hydroxide complexes in the present study suggest that chloride is firmly held in the binding pocket and does not exchange for adventitious hydroxide during workup. Further, only the Fe(III) axial hydroxide complex has displayed any evidence to undergo further reaction with Cu(II) to produce an as yet unidentified, possibly heterobinuclear compound.⁸²

In conclusion, two new configurationally stable CcO model compound ligands and several of their monometallic porphyrin complexes have been synthesized and characterized. There is general difficulty in forming bimetallic compounds with the present ligands, presumably due to inherent flexibility of the picket spacers, but there is some evidence that heterobinuclear compounds might be approached through an iron(III) hydroxo porphyrin intermediate. We continue to explore new synthetic strategies designed to expand the utility of such potentially binucleating picket-fence porphyrin ligands, while preserving the basic structural features that make them so appealing for modeling the CcO active site.

Acknowledgment. The Robert A. Welch Foundation (Grant C-0627) is gratefully acknowledged for support of this research.

Supporting Information Available: Synthetic procedures and experimental data for **2** and the Zn(II), Ni(II), and Cu(II) complexes of **1** and molar magnetic susceptibility versus temperature data for $[\text{Cu}^{\text{II}}\text{T}(\text{NAPOPY})_3\text{P}]$ and $[\text{Fe}^{\text{III}}\text{T}(\text{NAPOPY})_3\text{P}(\text{OH})]$. This material is available free of charge via the Internet at <http://pubs.acs.org>.

IC001274Q

- (67) Miyamoto, T. K.; Tsuzuki, S.; Hasegawa, T.; Sasaki, Y. *Chem. Lett.* **1983**, 1587.
 (68) Cheng, R.-J.; Latos-Grazynski, L.; Balch, A. L. *Inorg. Chem.* **1982**, *21*, 2412.
 (69) Harel, Y.; Felton, R. H. *J. Chem. Soc., Chem. Commun.* **1984**, 206.
 (70) Woon, T. C.; Shirazi, A.; Bruce, T. C. *Inorg. Chem.* **1986**, *25*, 3845.
 (71) Brewer, C. *Inorg. Chim. Acta* **1988**, *150*, 189.
 (72) Abu-Soud, H. M.; Silver, J. *Inorg. Chim. Acta* **1989**, *164*, 105.
 (73) Lexa, D.; Momenteau, M.; Saveant, J.-M.; Xu, F. *Inorg. Chem.* **1985**, *24*, 122.
 (74) Hambright, W. P.; Thorpe, A. N.; Alexander, C. C. *J. Inorg. Nucl. Chem.* **1968**, *30*, 3139.
 (75) Mitra, S. In *Iron Porphyrins*; Lever, A. B. P., Gray, H. B., Eds.; Addison-Wesley: Reading, MA, 1983; Vol. II, p 9.
 (76) Scheidt, W. R.; Geiger, D. K. *J. Chem. Soc., Chem. Commun.* **1979**, 1154.
 (77) Beattie, J. K.; West, J. R. *J. Am. Chem. Soc.* **1974**, *96*, 1933.
 (78) Dose, E. V.; Tweedle, M. F.; Wilson, L. J.; Sutin, N. *J. Am. Chem. Soc.* **1977**, *99*, 3886.
 (79) González, J. A.; Wilson, L. J. *Inorg. Chem.* **1994**, *33*, 1543 and references therein.
 (80) Gunter, M. J.; McLaughlin, G. M.; Berry, K. J.; Murray, K. S.; Irving, M.; Clark, P. E. *Inorg. Chem.* **1984**, *23*, 283.
 (81) Adler, A. D.; Longo, F. R.; Kampas, F.; Kim, J. *J. Inorg. Nucl. Chem.* **1970**, *32*, 2443.

- (82) Reaction of $[\text{FeT}(\text{NAPOPY})_3\text{P}(\text{OH})]$ with $\text{CuCl}_2 \cdot 2\text{H}_2\text{O}$ in $\text{CHCl}_3/\text{MeOH}$ produced a compound that gave a positive-ion FAB mass spectrum consistent with Cu incorporation ($M + 1 = 1216$).